IET Generation, Transmission & Distribution

Research Article

IET Journals
The Institution of Engineering and Technology

Distributed charging management of multi-class electric vehicles with different charging priorities

ISSN 1751-8687
Received on 3rd April 2019
Revised 2nd September 2019
Accepted on 9th October 2019
E-First on 30th October 2019
doi: 10.1049/iet-gtd.2019.0511
www.ietdl.org

Amro Alsabbagh[1], He Yin[2], Chengbin Ma[1] ✉

[1]*University of Michigan-Shanghai Jiao Tong University Joint Institute, 800 Dongchuan Road, Minhang District, Shanghai 200240, People's Republic of China*

[2]*Electrical Engineering and Computer Science, University of Tennessee, Knoxville, 411 Min H. Kao Building, 1520 Middle Drive, Knoxville, Tennessee 37996-001, USA*

✉ *E-mail: chbma@sjtu.edu.cn*

Abstract: This study proposes distributed energy management approach for charging multi-class electric vehicles (EVs) in community microgrids. The energy management problem is implemented in real-time and represented by a non-cooperative Stackelberg game for the power distribution inside the microgrid. In this game, a battery energy storage system is chosen as a leader and the EVs are designated as followers. The charging power distribution among EVs is tackled in the two cases of 'plenty of power' and 'lack of power'. The challenging case of 'lack of power' occurs when the total charging power is insufficient to meet the need of each EV, such as when weather conditions are unfavourable. A priority factor is included in the EV utility functions to address charging priorities of different classes of EVs in practical scenarios. A consensus-based distributed algorithm is developed later to iteratively reach the Nash equilibrium, i.e. final charging power distribution, among EVs with different charging priorities. Both simulation and experimental results show that the charging power is properly distributed when the predefined charging priorities are followed, particularly in the case of a 'lack of power'.

1 Introduction

The increasing environmental concerns have motivated the focus on microgrids (MGs) and electric vehicles (EVs). MGs are local power grid groupings of various distributed energy generators, energy storage devices, and loads (e.g. buildings and EVs). They can operate either in an islanded or a grid-connected mode [1]. Each component in an MG is expected to properly play its own role so that the MG can be fully functional in terms of natural resources (e.g. solar energy and wind energy) capture and storage, continuous power supply, and pollution mitigation. The very different dynamics and characteristics of the involved components, however, introduce the challenge of how to achieve effective and flexible energy management [2]. Further complicating energy managements are the significant charging power demands of EVs. With uncertainties in the number, types, capacities, and initial conditions of EVs, as well as the impact of users' behaviour, appropriate energy management strategies are highly desirable. Especially important in developing an effective energy management strategy is the need for flexibility and scalability in a dynamic environment.

The energy management problem related to EV charging in MGs has been widely studied in recent years. Current solutions to the problem can be classified into centralised and distributed approaches. One centralised solution involved a binary optimisation formulated for EV charging scheduling [3]. To improve computational efficiency for real-time implementation, a convex relaxation had been developed. However, this on–off charging strategy cannot provide continuous charging, and may potentially damage the on-board battery. Yan *et al.* [4] introduced a four-stage optimisation algorithm to reduce operational cost in an EV charging station, while balancing real-time supply and demand. No equations were provided to quantify the power flow among the major components of the charging station. In [5], an improved learning particle swarm optimisation algorithm was applied to optimise power distribution in an MG focusing on enhanced economic benefits. However, technical aspects were not fully discussed, such as charging power distribution among individual EVs and limited charging power capacity. Wu *et al.* [6] combined approximate dynamic programming and an evolution algorithm to determine the charging start time for each EV and thus reduce the operation cost of the charging station. The configuration of the charging system was relatively simple, and again there was no discussion on the cases with limited charging power capacity.

On the other hand, distributed approaches have the advantage of flexibility and scalability as well as lower communication bandwidth and computational effort. Zhao *et al.* [7] applied game theory to the context of an EV fast charging station. In this game theoretical approach, EVs act as followers of a system operator and decide how to optimise the trade-off between the benefits of charging and reserve provision. The work emphasised maximising social welfare instead of detailed charging power distribution among EVs. Garcia-Trivino *et al.* [8] presented a distributed control method for charging stations in which the control contains two independent fuzzy logic systems to maintain the dc bus voltage and SOC (state-of-charge) of ground battery energy storage system, and to keep the power balance stable among the charging station units. It lacked discussion on the practical cases with limited total charging power. Liu *et al.* [9] developed a real-time pricing scheme (i.e. an economic aspect) to minimise power distribution losses in plug-in EV (PEV) charging stations and to ensure system reliability. The preference of each PEV owner is modelled to satisfy his/her charging demand with minimised cost. Meanwhile, only the preferences of PEV owners were considered in the scheme, which simplified the actual interactions with other components. New developments included the application of the neurodynamic algorithm and hybrid distributed and centralised scheme to minimise the charging cost through a valley filling and to reduce photovoltaic (PV) curtailment, in which the possible insufficiency of the total available charging power was not addressed [10, 11]. Therefore, the purpose of this paper is to develop a real-time control scheme that (i) reflects the interactive relationship among EVs and other components, and (ii) addresses individual EV charging power distribution under limited total available charging power.

It is expected that improved interactions between EVs and MGs can be achieved by fully respecting the unique characteristics or preference of each individual component in the MG. To this end,

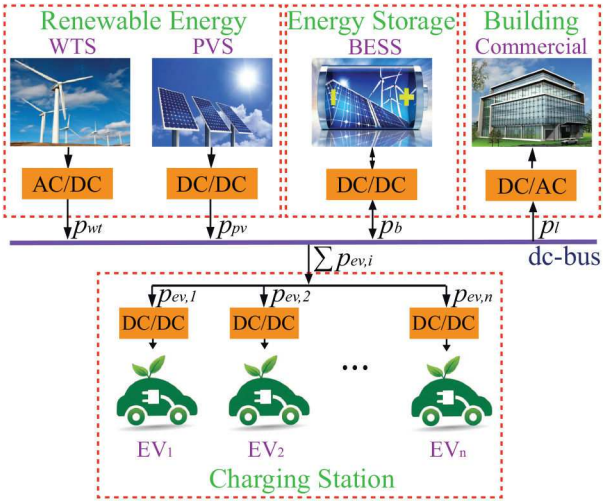

Fig. 1 *Example system configuration*

the components in an islanded-mode MG, which is more restrictive in terms of power distribution, are separately represented by independent players. The individual preference of each player is explicitly expressed through its own utility function. Due to the selfish nature of EV charging behaviours, a non-cooperative game theory is considered to be a suitable decision making tool. The advantage here is that the approach can represent the interactions among different EVs and the MG, solving the power distribution problem in a distributed manner. This approach is particularly relevant for the charging areas, where it will be of interest to assign categories or classes to EVs (i.e. multiple privilege levels for charging). A consensus-based distributed energy management algorithm is then developed to iteratively reach the so-called Nash equilibrium in game theory (i.e. balanced charging power distribution among EVs), particularly when there is a lack of power and plugged-in EVs have different charging priorities. Finally, both simulation and experiments are carried out to validate the proposed charging power distribution among multi-class EVs.

The major contributions of this paper are summarised as follows:

i. This paper extends the use of Stackelberg game in developing a real-time implementable energy management strategy for the power distribution inside an MG. Note that the Stackelberg game has been applied in the EV charging management problem, mostly with regard to its economic and social aspects, and scheduling [7, 12, 13].
ii. It tackles the EV charging power distribution problem in a 'lack of power' case, which is more dynamic than those in the existing demand curtailment request and overload control [3, 14].
iii. A priority factor is newly added to the utility function of each EV to address different classes of EVs. Unlike the existing literature that assigned the priority to EVs based on the balance between power demand and supply or the state parameters of EVs [15, 16], this classification is practically needed such as due to management purposes (e.g. workplace hierarchy and membership) or emergency response (e.g. EV ambulances operated by hospitals).

2 System configuration and modelling

As shown in Fig. 1, the example MG consists of a wind turbine system (WTS), a PV system (PVS), a battery energy storage system (BESS), a commercial building, and a charging station. Each component is connected to the dc bus through a compatible type of converter. Note that to investigate the case of a 'lack of power', which is challenging for power distribution, an islanded mode MG is chosen. However, this MG can also be switched to a grid-connected mode, such as through a bidirectional dc–ac inverter and transformer, and managed by straightforwardly extending the approach developed below.

The WT and PV models are derived as in [17], while the BESS is modelled by their equivalent circuit models. To fully utilise wind and solar energies, both the WTS and the PVS are operating in the maximum power point tracking (MPPT) mode. Since this paper focuses on EV charging, each EV $\in \mathcal{N}$ (number of plugged-in EVs) is represented by its on-board battery and charger (dc–dc converter). The on-board batteries can also be modelled using their equivalent circuit models. In the following simulation, the SOCs of both BESS and EV on-board batteries are updated based on the classical Coulomb-counting [18]. For the commercial building, a real-world profile (e.g. office) is taken [19]. Note that any other type of load profile, such as a residential or industrial one, can be also chosen. To reflect the realistic conditions of weather uncertainties, the Weibull distribution and the Beta distribution are chosen to represent wind speed and solar irradiance, respectively [20].

An actual MG has numerous constraints that reflect existing physical limitations (e.g. the dc-bus voltage and capacity of each component). To avoid redundancy, only the common equality constraint among all the components is highlighted here

$$p_{\mathrm{wt}} + p_{\mathrm{pv}} - p_{\mathrm{l}} - p_{\mathrm{b}} - \sum_{j=1}^{\mathcal{N}} p_{\mathrm{ev},i} = 0, \tag{1}$$

where the terms represent the powers generated or consumed by the WTS (p_{wt}), the PVS (p_{pv}), the commercial building (p_{l}), the BESS (p_{b}), and the ith EV ($p_{\mathrm{ev},i}$). As shown in Fig. 1, the relationship in (1) exists because the above terms are the powers flowing through the common dc bus. The line loss is assumed to be neglectable in the example MG. Obvious power losses occur during the conversions and battery charge/discharge, which may range between 5 and 15% of the total power. This affects the available p_{wt} and p_{pv}, and desired/preferred p_{l}, p_{b}, and $p_{\mathrm{ev},i}$.

3 Energy management

The aim of this paper is to develop a general and scalable approach for the charging management of multi-class EVs. A non-cooperative generalised Stackelberg game, in which the leader moves first and then the followers move sequentially, is utilised to model the strategic interactions in the present energy management problem [7, 12, 13]. In this game, the ground BESS is set to be a 'leader' because it is a major and controllable energy source for charging, while the EV charging systems (EVCSs), energy consumers, are designated as 'followers'. In real applications, the number of plugged-in EVs, i.e. active EVCSs, along with their SOCs and the SOC of the BESS may change over time. Thanks to its distributed nature, the proposed approach is particularly advantageous in private information protection, scalability, and computational efficiency, as discussed and validated in the following sections.

3.1 Utility functions

The commonly used concave quadratic form is selected to describe the preferences of the players, i.e. the BESS and the EVCSs, because the form allows a negotiable solution based on variable marginal effects [12, 21].

• *The BESS:* The preference of the BESS is defined for it to be properly charged and discharged, which maximises the following utility function:

$$u_{\mathrm{b}} = -(p_{\mathrm{b}} - p_{\mathrm{b}}^{\mathrm{opt}})^2, \tag{2}$$

with

$$p_{\mathrm{b}}^{\mathrm{opt}} = \begin{cases} (\mathrm{SOC}_{\mathrm{b}}^{\max} - \mathrm{SOC}_{\mathrm{b}}) P_{\mathrm{b}}^{\max} & \mathcal{N} = 0 \\ -(\mathrm{SOC}_{\mathrm{b}} - \mathrm{SOC}_{\mathrm{b}}^{\min}) P_{\mathrm{b}}^{\max} & \mathcal{N} > 0, \end{cases} \tag{3}$$

where $\mathcal{N}$ is the number of the plugged-in EVs; $p_{\mathrm{b}}^{\mathrm{opt}}$ is the desired power of the BESS that is inversely proportional to its $\mathrm{SOC_b}$. $\mathrm{SOC_b^{min}}$ and $\mathrm{SOC_b^{max}}$ are the minimum and maximum allowed SOCs; $P_{\mathrm{b}}^{\mathrm{max}}$ is the maximum charging/discharging power of the BESS. The BESS is expected to be charged when no EVs are plugged in, and discharged when they are. It helps to buffer the power and utilise it during the intermittence or lack of the generated power by the WTS and the PVS.

• *The EVCS:* This system consists of a charging pole along with a plugged-in EV. Note that in this context, the EVCSs and the EVs are used interchangeably. If there is a sufficient generated power, it is desirable for each EV to be charged following its charging power preference during bulk charge, i.e. when the SOC of the on-board battery is lower than a specific percentage. The EVCS utility function below is specifically designed for cases when the EVs have to compete for limited total available charging power, i.e. realistic cases of a lack of power

$$\begin{aligned} u_{\mathrm{ev},i} &= \alpha_{\mathrm{ev},i}\left[-\frac{1}{2}p_{\mathrm{ev},i}^2 + \frac{P_{\mathrm{ev},i}^{\mathrm{ref}}}{0.2}(1-\mathrm{SOC}_{\mathrm{ev},i})p_{\mathrm{ev},i}\right] \\ &= \alpha_{\mathrm{ev},i}\left[5P_{\mathrm{ev},i}^{\mathrm{ref}}(1-\mathrm{SOC}_{\mathrm{ev},i}) - \frac{1}{2}p_{\mathrm{ev},i}\right]p_{\mathrm{ev},i}\,. \end{aligned} \tag{4}$$

The above utility function is formulated so that the two terms in the function share the same unit. In (4), $\mathrm{SOC}_{\mathrm{ev},i}$ is the SOC of the EV battery; $P_{\mathrm{ev},i}^{\mathrm{ref}}$ is the reference charging power of a specific EV during a bulk charge here when $\mathrm{SOC}_{\mathrm{ev},i}$ is lower than 80%($= 1 - 0.2$); $p_{\mathrm{ev},i}$ is the actual charging power of the EV; and $\alpha_{\mathrm{ev},i}$ is the priority factor, defined as faster charging at a higher value. As explained below, the term $(P_{\mathrm{ev},i}^{\mathrm{ref}}/0.2)(1-\mathrm{SOC}_{\mathrm{ev},i})$ is introduced to reflect the desired charging power of an on-board battery at its different SOC, i.e. the cases when $\mathrm{SOC}_{\mathrm{ev},i} \leq$80% and >80% here. For the utility function, (4),

i. A larger $p_{\mathrm{ev},i}$, the charging power, leads to a larger $u_{\mathrm{ev},i}$ because the quadratic function (4) always monotonically increases for increasing $p_{\mathrm{ev},i}$ under the physical relationship of $p_{\mathrm{ev},i} \leq P_{\mathrm{ev},i}^{\mathrm{ref}} < (P_{\mathrm{ev},i}^{\mathrm{ref}}/0.2)(1-\mathrm{SOC}_{\mathrm{ev},i})$ when $\mathrm{SOC}_{\mathrm{ev},i}$ is lower than 80%. Note that mathematically $(P_{\mathrm{ev},i}^{\mathrm{ref}}/0.2)(1-\mathrm{SOC}_{\mathrm{ev},i})$ is the charging power that maximises $u_{\mathrm{ev},i}$. Thus, again, if there is sufficient generated power, the EV is simply charged with its preference charging power during a bulky charge, i.e. $P_{\mathrm{ev},i}^{\mathrm{ref}}$. If, however, the $\mathrm{SOC}_{\mathrm{ev},i}$ is larger than 80%, $(P_{\mathrm{ev},i}^{\mathrm{ref}}/0.2)(1-\mathrm{SOC}_{\mathrm{ev},i})$ becomes smaller than $P_{\mathrm{ev},i}^{\mathrm{ref}}$ and eventually becomes zero when $\mathrm{SOC}_{\mathrm{ev},i}$ reaches 100%. Thus, $p_{\mathrm{ev},i}$ has a tendency to be as close to $(P_{\mathrm{ev},i}^{\mathrm{ref}}/0.2)(1-\mathrm{SOC}_{\mathrm{ev},i})$ as possible because it maximises $u_{\mathrm{ev},i}$.
ii. Under a given $P_{\mathrm{ev},i}^{\mathrm{ref}}$ and $p_{\mathrm{ev},i}$, a lower $\mathrm{SOC}_{\mathrm{ev},i}$ results in a higher value of $u_{\mathrm{ev},i}$. Note that a lower on-board battery SOC means that the specific EV is more 'anxious' to be charged. Thus, with the same amount of charging power, that EV has a higher level of satisfaction than when its SOC is already high.
iii. Similarly, a larger $P_{\mathrm{ev},i}^{\mathrm{ref}}$ corresponds to a larger $u_{\mathrm{ev},i}$. Thus, an EV with a larger capacity on-board battery is more 'motivated' to compete for charging power.
iv. Finally, the priority factor $\alpha_{\mathrm{ev},i}$ scales $u_{\mathrm{ev},i}$. For the same EV, a larger $\alpha_{\mathrm{ev},i}$ results in a preferred status in terms of desired charging power. The priority factor, $\alpha_{\mathrm{ev},i}$, is added to the above utility function (4) to address different classes of EVs, such as those needed for emergency response or management purposes.

Note that the coefficient of the quadratic term, 1/2, is introduced to simplify the following derivations as in (10). In order to avoid padding in the context, the $_{\mathrm{ev}}$ notation in the subscript will be dropped in the following sections.

3.2 Solution of generalised Stackelberg game

For the leader, BESS, it is straightforward that

$$p_{\mathrm{b}} = p_{\mathrm{b}}^{\mathrm{opt}} + \Delta p, \tag{5}$$

where p_{b} is the final charging/discharging power of the BESS. Besides $p_{\mathrm{b}}^{\mathrm{opt}}$, physically the BESS must absorb Δp, surplus power beyond the charging powers required by the commercial building and the EVs [refer to the common constraint in (1)].

To charge EVs, however, there exists another game between the followers themselves, i.e. EVCSs, who share the inequality constraint (7)

$$p_{\mathrm{ava}} = p_{\mathrm{wt}} + p_{\mathrm{pv}} - p_{\mathrm{l}} - p_{\mathrm{b}}^{\mathrm{opt}}, \tag{6}$$

$$\sum_{i=1}^{\mathcal{N}} p_i \leq p_{\mathrm{ava}} \leq p_{\mathrm{dis}}, \tag{7}$$

where p_{ava} is the total charging power available for EVs considering the proper charge/discharge of the BESS (i.e. $p_{\mathrm{b}}^{\mathrm{opt}}$, the preference of the leader). Note that there is usually a physical limit on the capacity of charging power distribution inside an EV charging facility, p_{dis}, which is intuitively assumed to be larger than p_{ava} here. Meanwhile, this assumption does not change the essence of the present problem, namely a charging power distribution problem under limited total available charging power. This sub-game is a generalised Nash equilibrium (GNE) problem, in which all players need to reach the so-called Nash equilibrium in order to define the power distribution at each control instant. In this paper, the approach to finding the GNE is based on the Karush–Kuhn–Tucker (KKT) conditions of optimality and the Lagrange multipliers method, and thus the proposed Nash equilibrium here is in fact Pareto-optimal. The optimisation problem for each player is as follows:

$$\begin{aligned} &\mathrm{OBJ}: f_{\min} = -u_i \\ &\mathrm{s.t.} \sum_{i=1}^{\mathcal{N}} p_i - p_{\mathrm{ava}} \leq 0. \end{aligned} \tag{8}$$

The Lagrange function L is

$$L_i(p_i, \lambda_i) = -u_i + \lambda_i\left(\sum_{i=1}^{\mathcal{N}} p_i - p_{\mathrm{ava}}\right), \tag{9}$$

where λ_i is the Lagrange multiplier of each player. Let

$$\frac{\partial L_i}{\partial p_i} = \alpha_i\left[p_i - 5P_i^{\mathrm{ref}}(1-\mathrm{SOC}_i)\right] + \lambda_i = 0, \tag{10}$$

$$\frac{\partial L_i}{\partial \lambda_i} = \sum_{i=1}^{\mathcal{N}} p_i - p_{\mathrm{ava}} = 0. \tag{11}$$

The KKT conditions can then be directly solved, assuming all the EV related information are revealed. The most socially stable equilibrium is of interest and can be reached by requiring all λ_i's to have the same value, $\bar{\lambda}$ here [12]. If $\bar{\lambda}$ is zero, namely $\sum_{i=1}^{\mathcal{N}} p_i - p_{\mathrm{ava}} \leq 0$, simply

$$p_i = 5P_i^{\mathrm{ref}}(1-\mathrm{SOC}_i)\,. \tag{12}$$

Otherwise, for a common non-zero $\bar{\lambda}$, p_i can be solved as

$$p_i = \frac{p_{\mathrm{ava}} - 5\sum_{i=1}^{\mathcal{N}}\left[P_i^{\mathrm{ref}}(1-\mathrm{SOC}_i)\right]}{\alpha_i\sum_{i=1}^{\mathcal{N}}\frac{1}{\alpha_i}} + 5P_i^{\mathrm{ref}}(1-\mathrm{SOC}_i)\,. \tag{13}$$

I. Initialization Phase

1: $\lambda_i = 0$ $\quad \forall i \in \mathcal{N}$
2: $\alpha_i = 1$ $\quad \forall i \in \mathcal{N}$
3: $p_i = P_i^{ini}$ $\quad \forall i \in \mathcal{N}$
4: **if** $\sum_{i=1}^{\mathcal{N}} p_i \leq p_{ava}$ **then**
5: Terminate
6: **end if**

II. Tuning Phase

7: **for** $\forall i \in \mathcal{N}$ **do**
8: **if** $\alpha_i > \alpha_i^{ref}$ **then**
9: $\alpha_i \Leftarrow \alpha_i - \varepsilon_0$
10: **end if**
11: **end for**

III. Triggering Phase

12: $p_1 \leftarrow p_1 - k_p \left(\sum_{i=1}^{\mathcal{N}} p_i - p_{ava} \right)$
13: $\lambda_1 \leftarrow \alpha_1 \left[5P_1^{ref}(1 - SOC_1) - p_1 \right]$

IV. Consensus Phase

14: **while** $max(|\lambda_i - \lambda_j|) > \varepsilon_1$ **do** $\quad \forall i, j \in \mathcal{N}$
15: $\lambda_i \leftarrow \lambda_i + \sum_{j \in N_i} w_{i,j}(\lambda_j - \lambda_i)$
16: **end while**
17: **for** $\forall i \in \mathcal{N}$ **do**
18: $p_i = 5P_i^{ref}(1 - SOC_i) - \frac{\lambda_i}{\alpha_i}$
19: $p_i \leftarrow max[min(p_i, P_i^{ref}), 0]$
20: **end for**

V. Checking Phase

21: **if** $\left| \sum_{i=1}^{\mathcal{N}} p_i - p_{ava} \right| \leq \varepsilon_2$ **then**
22: Terminate
23: **else**
24: Go back phase II
25: **end if**

Fig. 2 *Algorithm 1: CDEM*

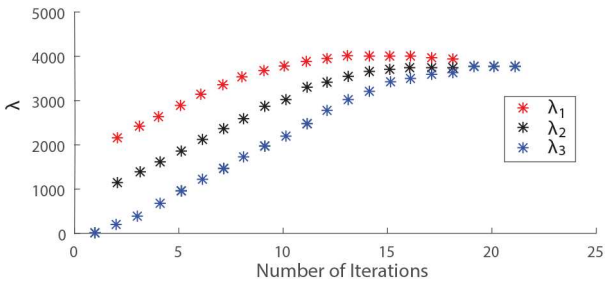

Fig. 3 *Example: number of iterations for convergence of λ_i's*

Table 1 Sizing of example system

Component	WTS	PVS	Load	BESS	$EV_{1,2,3}$
capacity	90 kWp	84.4 kWp	25 kWp	175 kWh	12, 24, 12 kWh

With the concave u_i's, both the existence and the uniqueness of the GNE can be mathematically proved.

As discussed in Section 1, the interest is in a distributed energy management approach that provides flexibility and scalability, secures the private information and lowers the complexity in computation in a dynamic environment. The aim in the proposed distributed approach is to let each player updates its demand repetitively until a uniform value of all λ_i's (i.e. $\bar{\lambda}$) is reached. To this end, the concept of consensus network will be utilised [21]. Intuitively, because of the distributed nature, there is an individual controller for each player, who shares only its own control variable (λ_i) rather than revealing all its internal parameters to others, such as SOC_i, P_i^{ref}, and α_i here. Thus, to reach the equilibrium state, one of the players is randomly selected to tune its own parameters so that it corresponds to the power mismatch, i.e. violating (7), as explained below. Without loss of generality, this random player will be indexed as '1'.

The attempt to reach the Nash equilibrium can be accomplished iteratively. This can be achieved by the proposed consensus-based distributed energy management (CDEM) algorithm, as shown in Algorithm 1 (see Fig. 2) for a single control instant. In the first step, an initialisation of all λ_i's, α_i's, and p_i's is performed, respectively, with zero value, an identical priority level such as one, preferred initial charging powers of the EVs P_i^{ini}, respectively, namely a preferred ideal case. If the available charging power p_{ave} is sufficient to meet all the P_i^{ini}'s, the algorithm simply terminates. Otherwise, a compromised solution has to be reached through a negotiation among the players, i.e. the EVCSs:

i. *Tuning phase:* The required charging power for the EVs is decreased by pulling them down to their predefined groups, i.e. classes. The priority condition will be checked and a step decrement of the EVs towards their reference priorities (α_i^{ref}) will be applied [refer to line 9].
ii. *Triggering phase:* A modification of λ_1, as a translation of the power mismatch will be carried out, as in lines 12 and 13. This shift in λ_1 will trigger an adjustment to the λ_i's and thus the plan for the distribution of charging power, as discussed in the next phase.
iii. *Consensus phase:* The aim of this stage is to converge all the values of λ_i's to a single one, $\bar{\lambda}$. This can be achieved by updating the λ_i of each node, utilising the sum of weighted differences between one node's λ_i and that of its neighbours' λ_j's as in line 15 [21]. N_i is the neighbour's set of node i, and $w_{i,j}$ is the connectivity strength between nodes i and j which should be chosen in the range $[0\,(1/N_i)]$ to ensure the intended convergence. When the desired convergence is achieved, the charging power distribution among the players will be assigned accordingly within the local boundaries, i.e. $p_i \leq P_i^{ref}$ [refer to line 19].
iv. *Checking phase:* The validity of the common constraint will be checked. The algorithm will reach the Nash equilibrium when the constraint is satisfied. Otherwise, the algorithm will return to the above three phases for modification to further suppress and lower the EV charging power currently demanded in order to meet the common constraint.

It is worth mentioning that in the above algorithm, the local information for a specific EVCS, α_i, P_i^{ref}, and SOC_i, does not need to be public. Only λ_i is shared among the other EVCSs [refer to lines 13, 15, and 18 in Algorithm 1 (Fig. 2)]. This advantage is especially useful for improving the flexibility and scalability of the charging management, and protect private information. Note that the values of ε_0, ε_1, and ε_2 are user defined, with better resolution at lower values sacrificing more iterations to reach convergence. Fig. 3 illustrates an example of the convergence of λ_i's after the triggering phase in the realistic case presented in Section 4.2, consisting of three EVs. As can be seen, the convergence is fast enough to be implemented in real time.

4 Simulation results

This paper investigates in detail the EV charging power distribution in real time. Showing the power distribution among a large number of EVs is realistic but may distract the focus of the discussion. Instead, a small-scale case study is first introduced for explanation purposes. A dedicated subsection is added later to especially investigate the scalability of the proposed approach when there is a large number of EVs. Thus, three EVs are first chosen as an example, and the size of the system is accordingly listed in Table 1 following the below guidelines:

i. The number of WT and PV modules meet the total load demand, i.e. the commercial building and the EVs loads here.
ii. The ratio between the WT and PV modules depends on criteria, such as the setup cost and the abundance of wind and solar energy.
iii. The capacity of the BESS mostly covers the cumulative difference between the generated and the consumed powers. Thus, the BESS buffers the power at the surplus generated power periods and utilises it during the intermittence or shortage periods of generated power.

The priority factors of the three EVs, EV_{1-3}, are chosen with different levels (i.e. classes), 0.75, 1, and 0.63, respectively. Again, the larger the number, the higher the charging priority. These three example priority factor levels are determined to enable a similar amount of differences in charging power. Note that in real applications, the priority factor for a specific EV could be assigned by the charging facility management company based on real needs. The sampling interval for the computation is chosen as 1 min, which is common in energy management [22].

4.1 Baseline case–plenty of power

A baseline 'plenty of power' case is designed to verify the system sizing given in Table 1 and to serve as a reference for comparison with the following 'lack of power' case. Three EV arrival time scenarios are created: morning (S_1: 8:00–10:00 AM), afternoon (S_2: 1:00–3:00 PM), and evening (S_3: 6:00–8:00 PM) [14]. As an example of the distributed arrivals of EVs in each scenario, one-hour interval is set, for instance 8:00, 9:00, and 10:00 AM in S_1. The initial SOCs of the EVs arriving for charging are 0.3, 0.25, and 0.2, respectively, i.e. low SOCs. To protect the on-board batteries, the desired ending SOC of the EVs is considered to be 90% [21]. The time a specific EV spends at the charging station can be straightforwardly calculated based on its initial and final SOCs, the capacity of the on-board battery, and the distributed charging power. Note that here all the EVs are supposed to be fully charged, i.e. with 90% ending SOC, before departure. Meanwhile, the proposed approach is capable to manage the cases with arbitrary departure time of the EVs because it is again a charging power redistribution problem. At the end of the following subsection, Section 4.2, a case with different EV ending SOCs is discussed and solved for verification purposes.

Figs. 4*a* and *b* show the power and SOC responses of all the involved major components throughout one day i.e. 24 h. In Fig. 4*a*, the dynamics of the power generated by the WTS and the PVS and the power consumed by the commercial building follow the distribution functions and profile mentioned in Section 2. The BESS in the three scenarios differs in its power responses due to the different BESS–EV interactions, i.e. different EV arrival times. All of the EVs are charged following the prescribed profile given in Section 3.1.

As shown in Fig. 4*b*, the SOC responses of the BESS reflect its mission to meet the load demands from the commercial building and EV charging. The difference in the SOCs in the above three scenarios is again due to the different arrival times of the EVs. Note that the final value of the BESS SOC matches the initial one, 0.45. This result indicates the appropriateness of the system sizing design in Table 1. In this 'plenty of power' case, the EVs are charged following their respective preferred charging profiles [refer to Section 3.1]. Their durations at the charging station are listed in the rows designated as '*CT*' (charging time) in Table 2.

4.2 Effect of priority factor–lack of power

When weather conditions are uncertain, there may be a lack of power. In such cases, some EVs may need to be charged with a higher priority, for instance, vehicles needed for emergencies or management purposes. This special need is represented in the EVCS utility function, (4), by the priority factor, $\alpha_{ev,i}$ or α_i afterwards. This priority factor scales the EVCS utility function and thus gives the high priority EVs a preferred status over others to enlarge their portions of the total available charging power. Of interest here is that, the class of an EV can be identified by the charging pole through a membership card or a communication protocol.

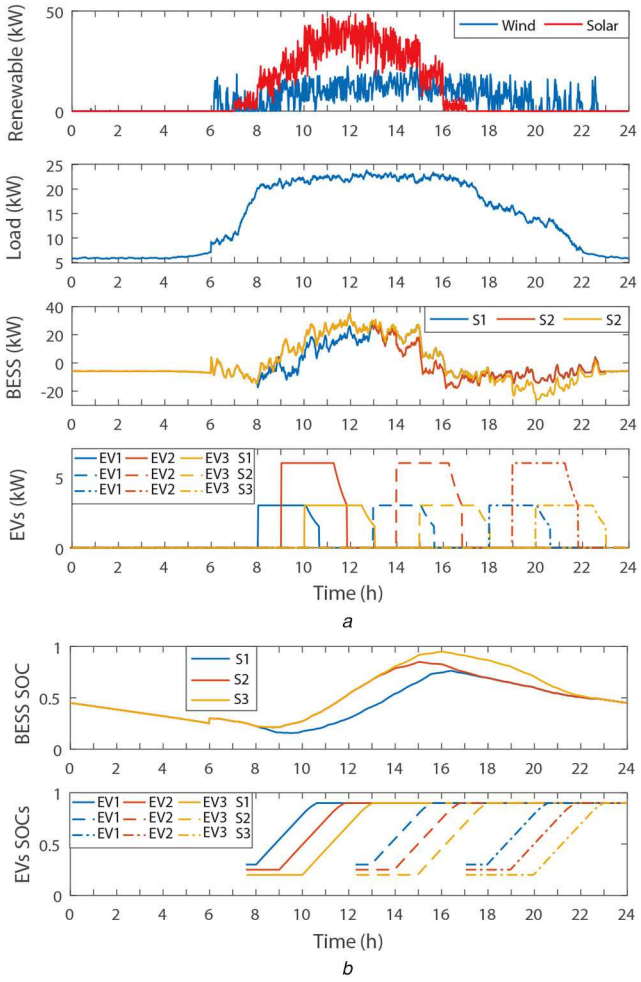

Fig. 4 *Responses in scenarios of S_1, S_2, and S_3*
(a) Power (kW), ***(b)*** SOC

Table 2 Comparison of two iterative methods

Criterion	EV	Plenty of power		Lack of power	
		Cen.	Dis.	Cen.	Dis.
CT, min	EV_1	158	158	366	366
	EV_2	170	170	250	250
	EV_3	182	182	258	258
ET_{avg}, s	EV_1	0.0191	0.0015	0.0234	0.0022
	$EV_{1,2}$	0.0222	0.0017	0.0451	0.0024
	$EV_{1,2,3}$	0.0412	0.0019	0.0563	0.0026
	EV_{1-100}	3.26	0.0121	5.56	0.3931

Table 3 Total available power for EV charging

Time, h	12:00–13:00 PM	13:00–15:00 PM	15:00–18:00 PM
p_{ava}, kW	18	15	10

In order to highlight the influence of the priority factor, the arrival times, SOCs and capacities of the on-board batteries of all three EVs are unified, 12:00 PM, 0.2, and 24 kWh. As explained in line 18 of the CDEM algorithm, p_i increases with a larger α_i under given P_i^{ref}, SOC_i, and λ_i. As shown in Table 3 and Fig. 5, in order to clearly investigate responses, the two cases of 'plenty of power' and 'lack of power', i.e. the cases of $\sum p_i \le p_{ava}$ and $\sum p_i \ge p_{ava}$, are included in the newly designed power profile.

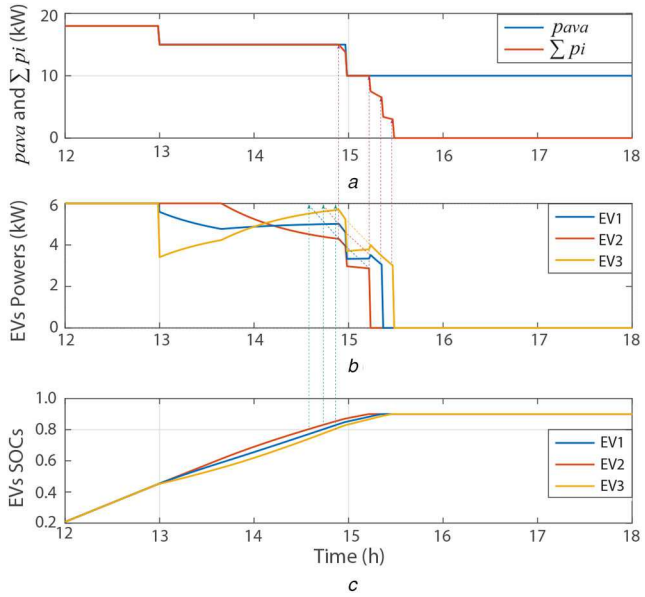

Fig. 5 *EVs' power and SOC responses under different priority levels*
(a) Total available charging power and sum of EVs' powers (kW), ***(b)*** EVs' powers (kW), ***(c)*** EVs' SOCs

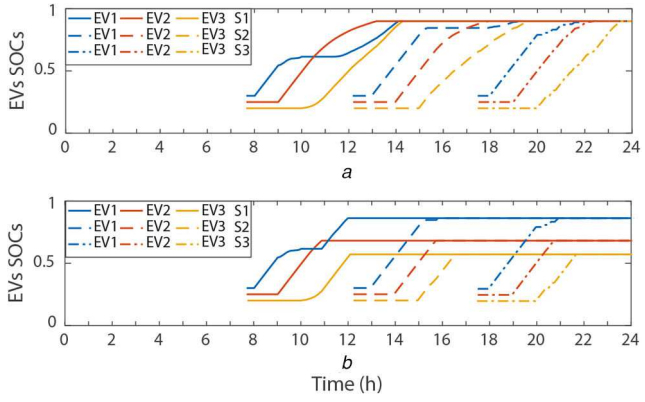

Fig. 6 *SOC Responses of EVs in S_{1-3} under a downscaled power profile*
(a) The same desired ending SOC (=0.9) for all EVs, ***(b)*** Different ending SOC (=0.86, 0.68, 0.57) for EV_1, EV_2, and EV_3, respectively

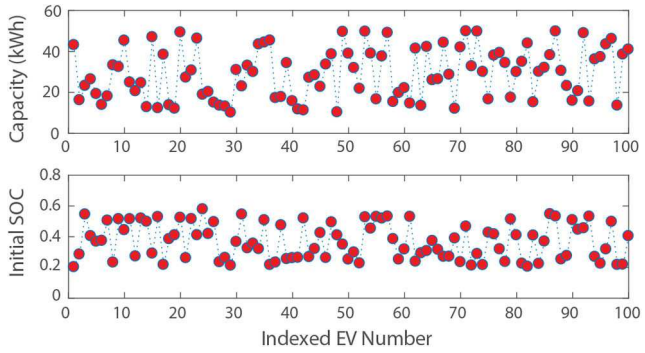

Fig. 7 *Example: distribution of battery capacities and initial SOCs of 100-EV case*

As shown in Fig. 5, during the first period, i.e. 12:00–13:00 PM, p_{ava}(=18 kW) rightly equals the sum of the optimal charging powers of the EVs. Thus, all three EVs are charged with their optimal power levels. From 13:00 to 15:00 PM, as p_{ava} decreases to 15 kW, which is below the sum of the optimal EV powers, i.e. there is a lack of power. The difference in the priority factors starts to have an influence. Meanwhile, as discussed below the final charging power of the EVs is dynamically determined according to the interactive relationship between the priority factors and the present battery SOCs [again refer to (4)].

Starting from 13:00 PM, the EV charging power distribution follows the different priority levels of the three EVs. The charging power of EV_3 is the lowest, but it increases because it has the lowest battery SOC of the three EVs. Similarly, the increasing and highest SOC of EV_2 causes it to gradually become less 'anxious' to compete for the limited charging power. This provides an opportunity for EV_1 and EV_3 to increase their share of the available charging powers. EV_3 eventually acquires the highest charging power due to its lowest SOC. In contrast, the highest SOC of EV_2, however, causes its charging power to drop to the lowest, despite its highest charging priority. All the above charging behaviours well follow the definition in (4) and match the needs of real applications. Note that the reference charging profile shown in Fig. 4*a* works any time the total supplied charging power is sufficient, e.g. before 15:00 PM. When p_{ava} suddenly drops to 10 kW at 15:00 PM, however, the lack of power reappears. After EV_2 quits charging (SOC≥0.9), p_{ava} becomes sufficient for the two remaining EVs to follow their reference charging profiles.

For further verification, the realistic wind and PV power profiles in Fig. 4 are modified to create a case of 'lack of power', as could occur during unfavourable weather conditions. Taken S_1 for instance, the wind power and commercial load power are assumed to be zero. The power from the PVS is scaled down by a factor of 0.15. The initial SOC of the BESS at 6:00 AM is set to be 0.2, rather than 0.3 as in the above section, to make the charging power distribution more challenging too, and thus better validate the proposed approach. The arrival times, battery capacities and initial SOCs of the three EVs in Section 4.1 are applied again. To avoid redundancy, only the EV SOCs are shown in Fig. 6*a*. The SOC responses are quite different from those in the baseline [see Fig. 4*b*]. As expected, as the highest priority, EV_2 is the first EV to be fully charged, even though it actually arrives at the charging station later than EV_1. EV_1's charging slows down significantly when EV_2 plugs in, and resumes again when the battery SOC of EV_2 is sufficiently high. When EV_3 joins the charging, the SOCs of EV_1 and EV_2 are already high. This provides capacity to charge EV_3 largely following its ideal charging profile. Different ending SOCs, 0.86, 0.68, and 0.57, for EV_1, EV_2, and EV_3, have also been chosen, respectively, namely the case with arbitrary EV departure time, and the EV SOC responses are shown in Fig. 6*b*. For comparison purposes, the simulation results of S_2 and S_3 scenarios are also shown in Fig. 6, in which a similar trend is observed. The same as for S_1, the wind and PV power profiles are adjusted accordingly to create the case of 'lack of power'. Note that here the BESS SOC varies between 0.2 and 0.3 in the three scenarios. The BESS is slightly charged through the down-scaled PVS and/or WTS, and then discharged due to the EV charging. In terms of energy management, the influence of this low remaining energy level of the BESS is equivalent with that of an insufficient battery capacity.

4.3 Scalability

Because of its distributed nature, the proposed approach is particularly advantageous in terms of scalability. For clarity of the explanation, the above case studies of the three EVs are used. However, the approach itself is general in that it can handle cases with even more EVs. The number of EVs is increased from 3 to 100. A100-run Monte Carlo simulation is adopted to investigate the average number of iterations to reach convergence in 'lack of power' cases. A random on-board battery capacity is chosen for the EVs, considering a normal distribution, 10–50 kWh [23]; the initial EV SOC values are again considered to follow a normal distribution, 0.2–0.6 [24] [see Fig. 7]. As shown in Fig. 8, the increase in the number of iterations does not follow an exponential growth. This observation validates the scalability when dealing with cases of a large number of EVs.

4.4 Computational efficiency

For reference purposes, the proposed distributed (Dis.) approach is compared with its centralised (Cen.) counterpart, taking S_1 as an

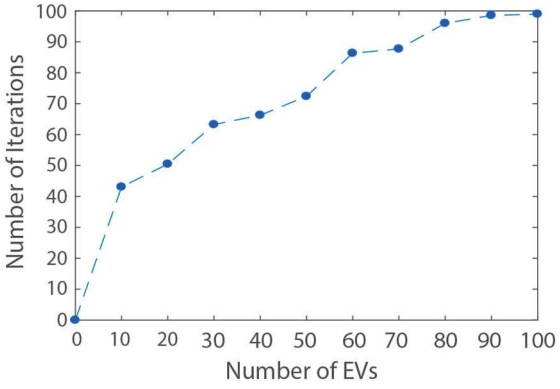

Fig. 8 *Number of iterations versus number of EVs in scalability analysis*

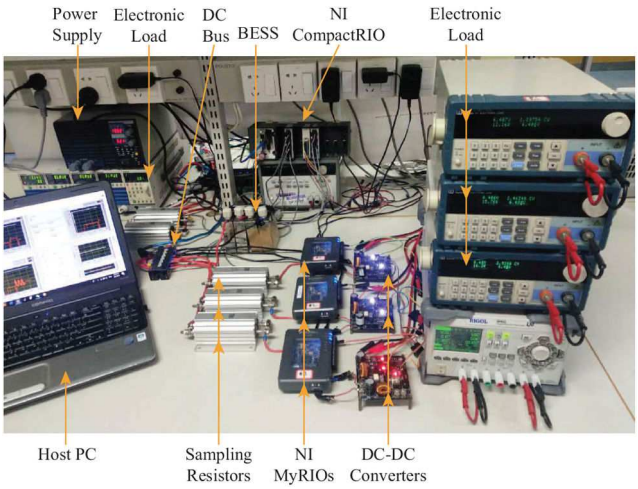

Fig. 9 *Downscaled testbed*

example. The constrained non-linear optimisation problem is solved via the sequential quadratic programming (SQP), an iterative but centralised method [25]. Two quantitative criteria are chosen for the evaluation, charging time (*CT*) to fully charge an EV and average execution time (ET_{avg}) for the algorithm code. The simulation setup is Matlab platform running on a personal computer (PC) with a 64-bit, dual core processor (2 GHz), and 6 GB RAM. As shown in Table 2, the *CT*s of the two iterative methods are identical, which validates the correctness of the results of the distributed approach; while the results are quite different for ET_{avg} when managing the charging of a single EV (EV_1), two EVs ($EV_{1,2}$), and then three EVs ($EV_{1,2,3}$). Similarly, in the above 100-EV case, ET_{avg} of the distributed approach is much smaller than that of the centralised approach. The distributed iterative approach shows an obviously improved computational efficiency, particulary when the number of EVs is large.

5 Experimental verification

A downscaled testbed, 1:550 at power level, is setup to validate the distributed implementation of the proposed charging management. As shown in Fig. 9, the WTS and the PVS are combined and emulated through a controllable power supply on the left side, while on the same side, the load of the commercial building is emulated by the electronic load. The BESS is set up using actual cells. The BESS is connected directly to the dc bus. The emulated EV charging facility on the right side contains three poles. Each pole consists of its own unidirectional buck dc–dc converter, electronic load to mimic the on-board battery dynamics, and a local National Instruments (NI) myRIO controller. The host PC collects and records all the experimental data as well as communicates with the NI CompactRIO and NI myRIOs via Ethernet and Wi-Fi, respectively. The host PC also controls all of the power supplies and electronic loads through its RS232 serial communication ports. All of the dc–dc converters are controlled by PI (proportional and

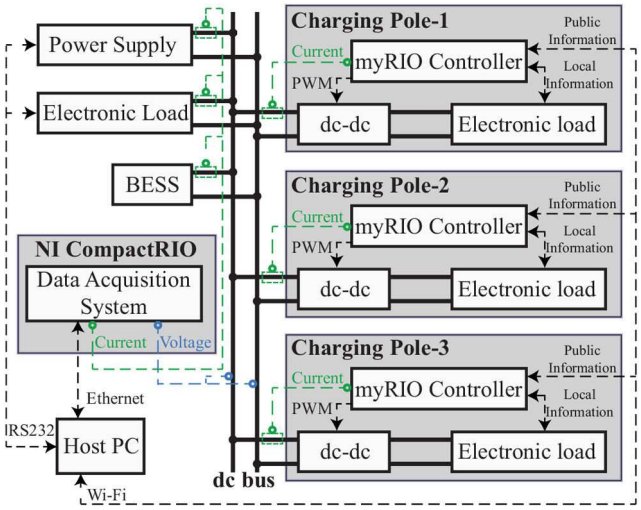

Fig. 10 *Functional blockdiagram of the testbed*

Table 4 Specifications for major components

Power Supply (Takasago ZX-800L)	Max power: 800 W (0–80 V, 0–80 A)
electronic load [left] (1 Kikusui PLZ-50F/150U)	max power: 600 W (1 PLZ-50F, 4 PLZ150USs with 1.5–150 V, 0–30 A each)
electronic loads [right] (3 Maynuo M9711)	max power: 150 W each (0–150 V, 0–30 A each)
dc–dc converters (design/fabricated in house)	max power: 100 W each switch frequency: 20 kHz
Li-ion battery pack (BESS) (Lishen LP2770102AC)	four cells (series), 12.5 Ah/cell, 3.2 V/cell (nominal voltage)
high-accuracy sampling resistors (PCN corporation RH series)	RH250M4 0.01 Ω (± 0.02%)

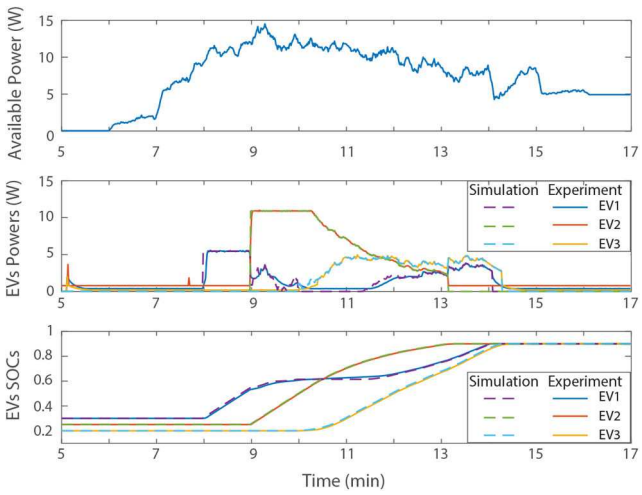

Fig. 11 *Experimental versus simulation results with a scaled time*

integral)-based pulse-width-modulation. The high-accuracy sampling resistors (±0.02%) are used as current sensors. Based on the above description, the functional block diagram of the testbed is shown in Fig. 10. The specifications for the major components of the testbed are listed in Table 4.

In order to conserve space, the experimental and simulation results are shown in Fig. 11, taking the realistic 'lack of power' case in the second half of Section 4.2 as an example. Experimental results, the EV charging powers, and SOCs, well match the results in the simulation. This validates the real-time implementation and correctness of the distributed charging management when EVs arrive at different times and with different charging priorities. The

efficiencies of the dc–dc converters, from which the most power losses occur in the present setup, are about 90%.

6 Conclusion

In order to handle emergencies and to ensure effective charging management of community microgrids, priority may need to be given to the charging of specific classes of EVs, particularly when the available charging power is insufficient, such as when weather conditions are unfavourable. This EV charging management problem can be represented by a non-cooperative Stackelberg game. In this game, the BESS is treated as a leader because it is a major energy source, while EVs are designated as followers. The different charging preferences of the two types of players are quantified on the basis of utility functions. Included in the utility functions of EVs are priority factors that define the classes of EVs in terms of charging. The consensus-based distributed algorithm is then developed to iteratively reach the Nash equilibrium (i.e. a balanced solution to the charging power distribution problem) among the multi-class EVs. The proposed distributed approach improves flexibility and scalability, secure private information, and significantly lower the required computational burden, together with reflecting the actual need to assign classes for EV charging. This practical idea of prioritising the charging of different classes of EVs could be extended to other contexts, such as taking into account different types or behaviours of EV drivers in charging management.

7 References

[1] Ravichandran, A., Sirouspour, S., Malysz, P., *et al.*: 'A chance-constraints-based control strategy for microgrids with energy storage and integrated electric vehicles', *IEEE Trans. Smart Grid*, 2018, **9**, (1), pp. 346–359

[2] Yoldaş, Y., Önen, A., Muyeen, S., *et al.*: 'Enhancing smart grid with microgrids: challenges and opportunities', *Renw. Sust. Energy Rev.*, 2017, **72**, pp. 205–214

[3] Yao, L., Lim, W.H., Tsai, T.S.: 'A real-time charging scheme for demand response in electric vehicle parking station', *IEEE Trans. Smart Grid*, 2017, **8**, (1), pp. 52–62

[4] Yan, Q., Zhang, B., Kezunovic, M.: 'Optimized operational cost reduction for an EV charging station integrated with battery energy storage and PV generation', *IEEE Trans. Smart Grid*, 2019, **10**, (2), pp. 2096–2106

[5] Qi, J., Lai, C., Xu, B., *et al.*: 'Collaborative energy management optimization toward a green energy local area network', *IEEE Trans. Ind. Inf.*, 2018, **14**, (12), pp. 5410–5418

[6] Wu, Y., Ravey, A., Chrenko, D., *et al.*: 'Demand side energy management of EV charging stations by approximate dynamic programming', *Energy Convers. Manage.*, 2019, **196**, pp. 878–890

[7] Zhao, T., Li, Y., Pan, X., *et al.*: 'Real-time optimal energy and reserve management of electric vehicle fast charging station: hierarchical game approach', *IEEE Trans. Smart Grid*, 2018, **9**, (5), pp. 5357–5370

[8] Garcia-Trivino, P., Torreglosa, J.P., Fernandez-Ramirez, L.M., *et al.*: 'Decentralized fuzzy logic control of microgrid for electric vehicle charging station', *IEEE J. Emerg. Sel. Top. Power Electron.*, 2018, **6**, (2), pp. 726–737

[9] Liu, Y., Deng, R., Liang, H.: 'A stochastic game approach for PEV charging station operation in smart grid', *IEEE Trans. Ind. Inf.*, 2018, **14**, (3), pp. 969–979

[10] Zhao, Y., He, X., Yao, Y., *et al.*: 'Plug-in electric vehicle charging management via a distributed neurodynamic algorithm', *Appl. Soft. Comput.*, 2019, **80**, pp. 557–566

[11] Kikusato, H., Fujimoto, Y., Hanada, S., *et al.*: 'Electric vehicle charging management using auction mechanism for reducing PV curtailment in distribution systems', *IEEET Sustain. Energy*, 2019, doi: 10.1109/TSTE.2019.2926998

[12] Tushar, W., Saad, W., Poor, H.V., *et al.*: 'Economics of electric vehicle charging: a game theoretic approach', *IEEE Trans. Smart Grid*, 2012, **3**, (4), pp. 1767–1778

[13] Yang, H., Xie, X., Vasilakos, A.V.: 'Noncooperative and cooperative optimization of electric vehicle charging under demand uncertainty: a robust Stackelberg game', *IEEE Trans. Veh. Technol.*, 2016, **65**, (3), pp. 1043–1058

[14] Li, J., Li, C., Xu, Y., *et al.*: 'Noncooperative game-based distributed charging control for plug-in electric vehicles in distribution networks', *IEEE Trans. Ind. Inf.*, 2018, **14**, pp. 301–310

[15] Eldjalil, C.D.A., Lyes, K.: 'Optimal priority-queuing for EV charging-discharging service based on cloud computing'. 2017 IEEE Int. Conf. on Communications (ICC), Paris, France, 2017, pp. 1–6

[16] Kumar, K.N., Sivaneasan, B., So, P.L.: 'Impact of priority criteria on electric vehicle charge scheduling', *IEEE Trans. Transp. Electrif.*, 2015, **1**, (3), pp. 200–210

[17] Zhang, J., Li, K.J., Wang, M., *et al.*: 'A bi-level program for the planning of an islanded microgrid including caes', *IEEE Trans. Ind. Appl.*, 2016, **52**, (4), pp. 2768–2777

[18] Piller, S., Perrin, M., Jossen, A.: 'Method for state of charge determination and their applications', *J. Power Sources*, 2001, **96**, pp. 113–120

[19] 'Commercial load datasets', (http://en.openei.org/datasets/files/961/pub/), accessed 27 March 2019

[20] 'Renewable resource data center, national renewable energy laboratory', (http://www.nrel.gov/rredc/), accessed 27 March 2019

[21] Rahbari-Asr, N., Chow, M.Y.: 'Cooperative distributed demand management for community charging of PHEV/PEVs based on KKT conditions and consensus networks', *IEEE Trans. Ind. Inf.*, 2014, **10**, (3), pp. 1907–1916

[22] Kisacikoglu, M.C., Erden, F., Erdogan, N.: 'Distributed control of PEV charging based on energy demand forecast', *IEEE Trans. Ind. Inf.*, 2018, **14**, (1), pp. 332–341

[23] Zhang, T., Chen, X., Yu, Z., *et al.*: 'A monte carlo simulation approach to evaluate service capacities of EV charging and battery swapping stations', *IEEE Trans. Ind. Inf.*, 2018, **14**, (9), pp. 3914–3923

[24] Rahmani-Andebili, M., Mahmud, F.F.: 'An adaptive approach for PEVs charging management and reconfiguration of electrical distribution system penetrated by renewables', *IEEE Trans. Ind. Inf.*, 2018, **14**, (5), pp. 2001–2010

[25] Fletcher, R., Bomze, I.M., Demyanov, V.F., *et al.*: 'The sequential quadratic programming method' in '*Nonlinear optimization*' (Springer, Berlin, Germany, 2010)